# Complete roughness and conductivity corrections for Casimir force measurement

G. L. Klimchitskaya,[1,*] Anushree Roy,[2] U. Mohideen,[2,†] and V. M. Mostepanenko[1,‡]
[1]*Physics Department, Federal University of Praíba, Caixa Postal 5008, CEP 58059-970, João Pessoa, Paraíba, Brazil*
[2]*Department of Physics, University of California, Riverside, California 92521*
(Received 8 June 1999)

We consider detailed roughness and conductivity corrections to the Casimir force in the recent Casimir force measurement employing an atomic force microscope. The roughness of the test bodies—a metal plate and a sphere—was investigated with the atomic force microscope and the scanning electron microscope, respectively. It consists of separate crystals of different heights and a stochastic background. The amplitude of roughness relative to the zero roughness level was determined and the corrections to the Casimir force were calculated up to the fourth order in a small parameter (which is this amplitude divided by the distance between the two test bodies). Also the corrections due to finite conductivity were found up to fourth order in relative penetration depths of electromagnetic zero-point oscillations into the metal. The theoretical result for the configuration of a sphere above a plate taking into account both corrections is in excellent agreement with the measured Casimir force. [S1050-2947(99)05011-8]

PACS number(s): 12.20.Fv, 42.50.Lc, 61.16.Ch

## I. INTRODUCTION

The Casimir effect [1], which arises in bounded regions and in spaces with nontrivial topology is of great interest to specialists in the most diverse fields of physics—from statistical and atomic physics to elementary particle physics and cosmology. It explores the dependence of the vacuum polarization on the geometrical parameters of the quantization domain, leading to attractive and repulsive forces acting between the boundaries (see the review papers [2,3] and the monographs [4,5]).

A considerable amount of recent attention has been focused on experimental verification of the Casimir force law between metallic surfaces. The first experiment of this kind was performed more than 40 years ago [6] and provided qualitative confirmation of the Casimir prediction. Then over a period of years the force between dielectric test bodies was used to measure the Casimir force (see, e.g., [7,8] and the other references in [4,5]). During this period only one paper may be cited [9] where the Casimir force between the plate and the spherical lens covered by chromium layers was measured. It should be noted that chromium is a poor reflector for a large portion of the measured distances. In this paper, considerable attention has been given to the finite conductivity corrections to the Casimir force. Also the possible corrections due to surface roughness were discussed qualitatively. In all the earlier experiments only variants of the spring balance were used to measure the force.

In the paper [10] that sets the modern stage of the Casimir force measurements between metals, the distance range from 0.6 $\mu$m to 6 $\mu$m was investigated. The test bodies were Cu plus Au coated quartz, optical flat, and a spherical lens. The torsion pendulum was used to measure the Casimir force. As mentioned in [10], experimental data do not support the presence of finite conductivity corrections that are negative and can achieve 20% of the net Casimir force at the closest spacing. The roughness corrections that can achieve 20– 30 % of the net result if there are deviations of the interacting surfaces from the perfect shape [11] were not investigated in [10]. As discussed in [10] also, the data are not of sufficient accuracy to demonstrate the finite-temperature corrections. We would like to point out that the temperature correction at room temperature is 129% and 174% of the net force when the space separation is correspondingly 5 $\mu$m and 6 $\mu$m. The values of both the Casimir force and temperature correction to it at such distances are of the order of $10^{-12}N$. Their experimental measurement and investigation is the unresolved problem of paramount importance.

In [12] an atomic force microscope (AFM) was used to make a precision measurement of the Casimir force between a sphere and a flat plate covered by the Al and Au/Pd layers. The measurements were done for plate-sphere separations between 0.1 $\mu$m and 0.9 $\mu$m. The experimental data were shown to be consistent with the theoretical calculations, including the finite conductivity and roughness corrections calculated up to second order in appropriate parameters [13]. No account has been taken in these calculations of the specific shape of roughness peculiar to the test bodies in use. Also the third and fourth orders of these corrections were neglected, although they could contribute to the comparison of the theory and experiment at an accuracy level of 1% for the smallest separations (temperature corrections are not important in this distance range). Other techniques for measuring the Casimir force have also been proposed (see, e.g., [14,15]).

Here we present the complete experimental and theoretical investigation of the surface roughness and roughness corrections to the Casimir force in the experiment [12]. For this

*On leave from North-West Polytechnical Institute, St. Petersburg, Russia. Electronic address: galina@GK1372.spb.edu
†Electronic address: umar.mohideen@ucr.edu
‡On leave from A. Friedmann Laboratory for Theoretical Physics, St. Petersburg, Russia.
Electronic address: mostep@fisica.ufpb.br

 

purpose the roughness of the plate was measured with the AFM, and the roughness of the sphere by the scanning electron microscope (SEM). The surface is composed of large separate crystals situated irregularly on the surface. They are modeled by parallelepipeds of two different heights situated on the stochastic background. The corresponding corrections to the Casimir force are computed by the use of the approximate method proposed earlier in [16,17]. The corrections due to roughness up to fourth order in relative roughness amplitude are obtained.

To provide the higher-order finite conductivity corrections the measurement range is subdivided into ranges of small and large distances. It is shown that at small distances it is possible to neglect the external Au/Pd cap layer. At large distances the effective penetration depth of the electromagnetic zero-point oscillations into the metal is found. As a result the corrections due to finite conductivity up to the fourth order are calculated, taking into account the effect of the surface roughness. The resulting Casimir force with both corrections is in excellent agreement with the experimental data.

The paper is organized as follows. In Sec. II the necessary details of the experiment [12] are reviewed. Section III contains a brief formulation of the perturbative approach to the calculation of roughness corrections. In Sec. IV the investigation of surface roughness and the roughness corrections is presented in relation to the experiment [12]. Section V is devoted to the corrections due to the finite conductivity of the metals. Here, the final expressions for the Casimir force including both corrections are also obtained. In Sec. VI they are compared with the experimental data of [12]. Section VII contains conclusions and a discussion. Throughout the paper units, in which $\hbar = c = 1$, are used.

## II. MEASUREMENT OF THE CASIMIR FORCE

In Ref. [12] a standard AFM was used to measure the force between a metallized sphere and flat plate at a pressure of 50 mTorr and at room temperature. Polystyrene spheres of $200 \pm 4$ $\mu$m diameter were mounted on the tip of 300-$\mu$m-long cantilevers with Ag epoxy. A 1.25-cm-diam optically polished sapphire disk was used as the plate. The cantilever (with sphere) and plate were then coated with 300 nm of Al in an evaporator. Aluminum is used because of its high reflectivity for wavelengths (sphere-plate separations) $>100$ nm. Both surfaces were then coated with less than a 20-nm layer of 60% Au/40% Pd. The sphere diameter was measured using the SEM to be $196.0 \pm 0.5$ $\mu$m.

In the AFM, the force on a cantilever is measured by the deflection of its tip. A laser beam is reflected off the cantilever tip to measure its deflection. A force on the sphere would result in a cantilever deflection leading to a difference signal between photodiodes *A* and *B* (shown in Fig. 1). This force and the corresponding cantilever deflection are related by Hooke's law: $F = k\Delta z$, where $k$ is the force constant and $\Delta z$ is the cantilever deflection. The piezoextension with applied voltage was calibrated with height standards and its hysteresis was measured. The corrections due to the piezohysteresis (2% linear correction) and cantilever deflection (discussed in [12]) were applied to the sphere-plate separations in all collected data.

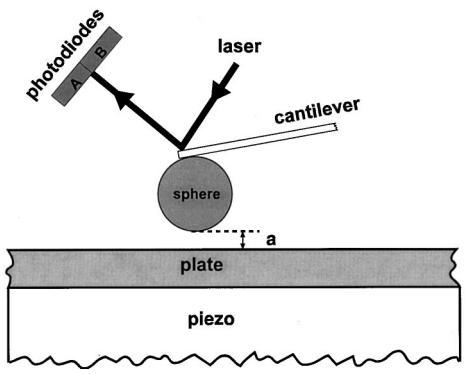


FIG. 1. Schematic diagram of the experimental setup. Application of voltage to the piezoelectric element results in the movement of the plate towards the sphere.

To measure the Casimir force between the sphere and the plate they are grounded together with the AFM. The plate is then moved towards the sphere in 3.6-nm steps and the corresponding photodiode difference signal is measured (approach curve). The signal obtained for a typical scan is shown in Fig. 2. Here ''0'' separation stands for contact of the sphere and plate surfaces. It does not take into account the absolute average separation between the Au/Pd layers due to the surface roughness, which is about 80 nm (see Sec. IV). If one also takes into account the Au/Pd cap layers that are transparent at small separations (see Sec. V) the absolute average separation at contact between Al layers is about 120 nm. Region 1 shows that the force curve at large separations is dominated by a linear signal. This is due to increased coupling of scattered light into the diodes from the approaching flat surface. Embedded in the signal is a long-range attractive electrostatic force from the contact potential difference between the sphere and plate, and the Casimir force (small at such large distances). In region 2 (absolute separations vary from contact to 350 nm) the Casimir force is the dominant characteristic far exceeding all the systematic errors. Region 3 is the flexing of the cantilever resulting from the continued extension of the piezoelectric element after contact with the two surfaces. Given the distance moved by the flat plate ($x$ axis), the difference signal of the photodiodes can be calibrated to a cantilever deflection in nanometers using the slope of the curve in region 3.

Next, the force constant of the cantilever was calibrated by an electrostatic measurement. The sphere was grounded to the AFM and different voltage in the range $\pm 0.5$ V to $\pm 3$ V were applied to the plate. The force between a charged sphere and plate is given as [18]

$$F = 2\pi\epsilon_0 (V_1 - V_2)^2 \sum_{n=1}^{\infty} \operatorname{csch} n\alpha (\coth\alpha - n \coth n\alpha). \tag{1}$$

Here $V_1$ is the applied voltage on the plate, $V_2$ represents the residual potential on the grounded sphere, and $\epsilon_0$ is the permittivity of free space. One more notation is $\alpha = \cosh^{-1}(1 + a/R)$, where $R$ is the radius of the sphere and $a$ is the separation between the sphere and the plate. From the difference in force for voltages $\pm V_1$ applied to the plate, we can measure the residual potential on the grounded sphere $V_2$ as

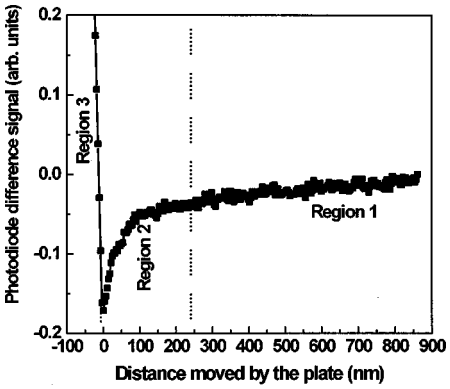


FIG. 2. Typical force curve as a function of the distance moved by the plate.

29 mV. This residual potential is a contact potential that arises from the different materials used to ground the sphere. The electrostatic force measurement was repeated at five different separations and for eight different voltages $V_1$. Using Hooke's law and the force from Eq. (1), we measure the force constant of the cantilever $k$. The average of all the measured $k$ is 0.0182 N/m.

The systematic error corrections to the force curve of Fig. 2, due to the residual potential on the sphere and the true separations between the two surfaces, are now calculated. Here the near linear force curve in region 1 is fit to a function of the form $F=F_c(a+a_0)+B/(a+a_0)+C\times(a+a_0)+E$. Here $a_0$ is the absolute separation at contact, which is constrained to $120\pm5$ nm, and is the only unknown to be completely obtained by the fit. The second term represents the inverse linear dependence of the electrostatic force between the sphere and plate for $R\gg a$, as given by Eq. (1). The constant $B=-2.8$ nN nm corresponding to $V_2=29$ mV and $V_1=0$ in Eq. (1) is used. The third term represents the linearly increasing coupling of the scattered light into the photodiodes and $E$ is the offset of the curve. Both $C$ and $E$ can be estimated from the force curve at large separations. The best-fit values of $C$, $E$, and the absolute space separation $a_0$ are determined by minimizing the $\chi^2$. The finite conductivity correction and roughness correction (the largest corrections) do not play a significant role in region 1 (see Sec. VI) and thus the value of $a_0$ determined by the fitting is unbiased with respect to these corrections. These values of $C$, $E$, and $a_0$ are then used to subtract the systematic errors from the force curve in regions 1 and 2 to obtain the measured Casimir force as $(F_c)_m=F_m-B/a-Ca-E$, where $F_m$ is the measured total force.

This procedure is repeated for 26 scans in different locations of the flat plate. The average measured Casimir force $(F_c)_m$ as a function of sphere-plate separations from all the scans is shown in Figs. 4 and 5 below as open squares.

## III. ROUGHNESS CORRECTIONS TO THE CASIMIR FORCE

For distances of $a\sim1$ $\mu$m between the interacting bodies the surface roughness makes an important contribution to the value of the Casimir force. Although an exact calculation of the roughness contribution is impossible, one can find the corresponding corrections approximately with the required accuracy. In the case of stochastic roughness the corrections to the van der Waals and Casimir forces were first calculated in [19] up to second order in relative roughness dispersions (the fourth order corrections were obtained in [20]). Effects of large-scale surface roughness on only the nonretarded van der Waals force were investigated in [21,22].

The method of greatest practical utility is the summation of retarded interatomic potentials over all atoms of two bodies distorted by roughness with a subsequent multiplicative normalization of the interaction coefficient [16,17]

$$U(a)=-\frac{CN_1N_2}{K}\int_{V_1}d\mathbf{r}_1\int_{V_2}d\mathbf{r}_2|\mathbf{r}_1-\mathbf{r}_2|^{-7}. \tag{2}$$

Here $N_{1,2}$ are the numbers of atoms per unit volume of the bodies, $C$ is the constant of the retarded van der Waals interaction, $K$ is a special normalization constant, and $a$ is a distance between bodies.

The appropriate choice of the normalization constant $K$ gives the possibility of increasing the accuracy of additive summation. Its value can be found as a ratio of the additive and exact potentials for the configuration admitting the exact solution. For two plane parallel plates, as an example that is most important for the experiment,

$$K=\frac{CN_1N_2}{\Psi(\varepsilon_1,\varepsilon_2)}>1, \tag{3}$$

where the $\Psi$ is defined as [23]

$$\Psi(\varepsilon_1,\varepsilon_2)=\frac{5}{16\pi^3}\int_0^\infty\int_1^\infty\frac{x^3}{p^2}\left\{\left[\frac{(s_1+p)(s_2+p)}{(s_1-p)(s_2-p)}e^x-1\right]^{-1}+\left[\frac{(s_1+p\varepsilon_1)(s_2+p\varepsilon_2)}{(s_1-p\varepsilon_1)(s_2-p\varepsilon_2)}e^x-1\right]^{-1}\right\}dp\,dx. \tag{4}$$

Here, $s_{1,2}=(\varepsilon_{1,2}-1+p^2)^{1/2}$, and $\varepsilon_{1,2}$ are the static dielectric permittivities of the plate materials.

From Eqs. (2) and (3) the Casimir force is

$$F=-\frac{\partial U}{\partial a},\quad U(a)=-\Psi(\varepsilon_1,\varepsilon_2)\int_{V_1}d\mathbf{r}_1\int_{V_2}d\mathbf{r}_2|\mathbf{r}_1-\mathbf{r}_2|^{-7}. \tag{5}$$

For the configuration of two plane parallel plates, Eq. (5) is exact by construction. We use here the word ''exact'' implying that the approximative method does not bring any additional error. Actually, the so-called ''exact'' results are obtained in the approximation of large distances with the proviso that $a\gg\lambda_0$, where $\lambda_0$ is the characteristic wavelength of absorption spectra. At the same time the values of $a$ must satisfy the condition $aT\ll1$, where $T$ is a temperature measured in energy units. For two plates, or a plate and a lens, or a sphere of large curvature radius covered by roughness, the relative error of the results obtained by Eq. (5) does not exceed $10^{-2}$% [17] (this is proved under the supposition that the roughness amplitude $A$ is much smaller than $a$). Because of this the proposed method is very useful for the calculation of the roughness contribution in experiments on the Casimir force.

Recently, other methods for approximative calculation of the Casimir force have been proposed. Among them the semiclassical [24] and macroscopic [25] approaches are applicable to the case of a sphere near a wall. They do not take into account the surface roughness. Also the path-integral approach was suggested [26] to study the space and time deformations of the perfectly reflecting boundaries. It was applied to describe the model example of corrugated plates when the lateral component of the Casimir force arises.

Now consider a plane plate (disk) of dimension $2L$, thickness $D$, and a sphere above it of radius $R$ both covered by roughness. The roughness on the plate is described by the function

$$z_1^{(s)}=A_1 f_1(x_1,y_1), \tag{6}$$

where the value of amplitude is chosen in such a way that $\max|f_1(x_1,y_1)|=1$. It is suitable to fix the zero point in the $z$ axis by the condition

$$\langle z_1^{(s)}\rangle=A_1\langle f_1(x_1,y_1)\rangle\equiv\frac{A_1}{4L^2}\int_{-L}^{L}dx_1\int_{-L}^{L}dy_1\,f_1(x_1,y_1)=0. \tag{7}$$

The roughness on the sphere is most conveniently described in the polar coordinates

$$z_2^{(s)}=a+R-\sqrt{R^2-\rho^2}+A_2 f_2(\rho,\varphi). \tag{8}$$

The value of the amplitude is chosen as specified above. The value of $R$ in Eq. (8) is defined in such a way that $\langle f_2(\rho,\varphi)\rangle=0$.

The potential $U$ from Eq. (5) for the configuration of a plate and a sphere with roughness described by Eqs. (6) and (8) can be represented as

$$U(a)=-\Psi(\varepsilon_1,\varepsilon_2)\int_0^{2\pi}d\varphi\int_0^{R}\rho\,d\rho\int_{z_2^{(s)}}^{a+2R}dz_2\,U_A(\rho,\varphi,z_2), \tag{9}$$

where

$$U_A(\rho,\varphi,z_2)=\int_{-L}^{L}dx_1\int_{-L}^{L}dy_1\int_{-D}^{z_1^{(s)}}\frac{dz_1}{[(x_1-\rho\sin\varphi)^2+(y_1-\rho\cos\varphi)^2+(z_1-z_2)^2]^{7/2}}. \tag{10}$$

In Ref. [11] the perturbation theory was developed in small parameters $A_{1,2}/a$ based on Eqs. (5), (9), and (10). All the results were obtained in zeroth order of the parameters $a/D$, $a/L$, and $a/R$, which are much smaller than $A_{1,2}/a$ (in Ref. [13] it was shown that the corrections due to the finiteness of a plate are negligible). The perturbation expansion for the Casimir force is

$$F_R(a)=F_0(a)\sum_{k=0}^{4}\sum_{l=0}^{4-k}C_{kl}\left(\frac{A_1}{a}\right)^k\left(\frac{A_2}{a}\right)^l, \tag{11}$$

where the force acting between the perfect plate and the sphere is

$$F_0(a)=-\Psi(\varepsilon_1,\varepsilon_2)\frac{\pi^2R}{15a^3}. \tag{12}$$

When the plate and the sphere are perfect metals we have the limiting case $\varepsilon_{1,2}\to\infty$, $\Psi\to\pi/24$ and Eq. (12) takes the form

$$F_0(a)=-\frac{\pi^3R}{360a^3}. \tag{13}$$

The first coefficient of Eq. (11) is $C_{00}=1$. The other coefficients were found in Ref. [11] for the configuration of a lens (sphere) above a plate and in Ref. [17] for two plane parallel plates. They are complicated integrals involving functions describing roughness. In the case in which

$$d_p,d_s\ll\sqrt{aR}, \tag{14}$$

where $d_p,d_s$ are the characteristic lateral sizes of distortions covering the plate and the sphere, the simple universal expression for the expansion coefficients of Eq. (11) can be obtained. As a result, Eq. (11) takes the form

$$\begin{aligned}F_R(a)=F_0(a)\Bigg\{1+6\Bigg[&\langle\langle f_1^2\rangle\rangle\left(\frac{A_1}{a}\right)^2-2\langle\langle f_1f_2\rangle\rangle\frac{A_1}{a}\frac{A_2}{a}\\&+\langle\langle f_2^2\rangle\rangle\left(\frac{A_2}{a}\right)^2\Bigg]+10\Bigg[\langle\langle f_1^3\rangle\rangle\left(\frac{A_1}{a}\right)^3-3\langle\langle f_1^2f_2\rangle\rangle\\&\times\left(\frac{A_1}{a}\right)^2\frac{A_2}{a}+3\langle\langle f_1f_2^2\rangle\rangle\frac{A_1}{a}\left(\frac{A_2}{a}\right)^2-\langle\langle f_2^3\rangle\rangle\left(\frac{A_2}{a}\right)^3\Bigg]\\&+15\Bigg[\langle\langle f_1^4\rangle\rangle\left(\frac{A_1}{a}\right)^4-4\langle\langle f_1^3f_2\rangle\rangle\left(\frac{A_1}{a}\right)^3\frac{A_2}{a}\\&+6\langle\langle f_1^2f_2^2\rangle\rangle\left(\frac{A_1}{a}\right)^2\left(\frac{A_2}{a}\right)^2-4\langle\langle f_1f_2^3\rangle\rangle\frac{A_1}{a}\left(\frac{A_2}{a}\right)^3\\&+\langle\langle f_2^4\rangle\rangle\left(\frac{A_2}{a}\right)^4\Bigg]\Bigg\}.\end{aligned} \tag{15}$$

Here the double angle brackets denote two successive averaging procedures. The first one is the averaging over the surface area of interacting bodies. The second one is over all possible phase shifts between the distortions situated on the surfaces of interacting bodies against each other. This second

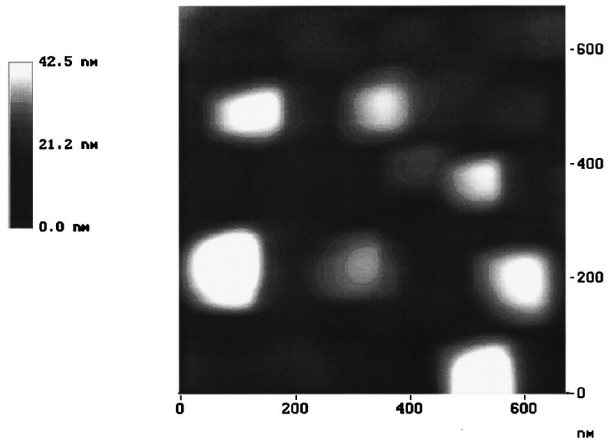


FIG. 3. Typical atomic force microscope scan of the metal surface. The lighter tone corresponds to larger height as shown by the bar graph on the left.

averaging is necessary because in the experiment [12] the measured Casimir force was averaged over 26 scans (see Sec. II).

Note that under condition (14) the result (15) can be obtained in two ways: starting from Eqs. (9),(10) for a sphere above a plate [11] and applying the force proximity theorem [27] to Eq. (25) of Ref. [17], which is an analog of Eq. (15) for the configuration of two plane parallel plates. As one would expect, the results coincide [in the case of large-scale roughness violating the condition (14) the special redefinition of a distance is needed for the correct application of the force proximity theorem [13]].

## IV. INVESTIGATION OF THE SURFACE ROUGHNESS

Let us apply the result (15) to carefully calculate the roughness corrections to the Casimir force in the experiment [12]. The roughness of the metal surface was measured with the same AFM. After the Casimir force measurement the cantilever with sphere was replaced with a standard cantilever having a sharp tip. Regions of the metal plate differing in size from $1\,\mu\mathrm{m}\times 1\,\mu\mathrm{m}$ to $0.5\,\mu\mathrm{m}\times 0.5\,\mu\mathrm{m}$ were scanned with the AFM. A typical surface scan is shown in Fig. 3. The roughness of the sphere was investigated with a SEM and found to be similar to the flat plate. In the surface scan of Fig. 3, the lighter tone corresponds to larger height.

As is seen from Fig. 3 the major distortions are the large separate crystals situated irregularly on the surfaces. They can be modeled approximately by the parallelepipeds of two heights. As the analysis of several AFM images shows, the height of the highest distortions is about $h_1=40$ nm, and that of the intermediate ones about $h_2=20$ nm. Almost all surface between the distortions is covered by the stochastic roughness of height $h_0=10$ nm. It consists of small crystals that are not clearly visible in Fig. 3 due to the vertical scale used. All together they form the homogeneous background of the averaged height $h_0/2$. The character of roughness on the plate and on the lens is quite similar. Note that in [12] only the highest distortions $h_1=40$ nm were used to estimate the distortion amplitude.

Now it is possible to determine the height $H$ relative to which the middle value of the function, describing the total roughness, is zero. It can be found from the equation

$$(h_1-H)S_1+(h_2-H)S_2-\left(H-\frac{h_0}{2}\right)S_0=0, \qquad (16)$$

where $S_{1,2,0}$ are, correspondingly, the surface areas occupied by distortions of the heights $h_1,h_2$ and stochastic roughness. Dividing Eq. (16) into the area of interacting surface $S=S_1+S_2+S_0$, one gets

$$(h_1-H)v_1+(h_2-H)v_2-\left(H-\frac{h_0}{2}\right)v_0=0, \qquad (17)$$

where $v_{1,2,0}=S_{1,2,0}/S$ are the relative parts of the surface occupied by the different kinds of roughness. The analysis of the AFM pictures similar to Fig. 3 gives us the values $v_1=0.11$, $v_2=0.25$, $v_0=0.64$. Solving Eq. (17) we get the height of the zero-distortion level $H=12.6$ nm. The value of the distortion amplitude defined relatively to this level is

$$A=h_1-H=27.4\,\mathrm{nm}. \qquad (18)$$

Below, two more parameters will also be used:

$$\beta_1=\frac{h_2-H}{A}\approx 0.231, \quad \beta_2=\frac{H-h_0/2}{A}\approx 0.346. \qquad (19)$$

With their help the distortion function from Eq. (6) can be represented as

$$f_1(x_1,y_1)=\begin{cases}1, & (x_1,y_1)\in\Sigma_{S_1},\\ \beta_1, & (x_1,y_1)\in\Sigma_{S_2},\\ -\beta_2, & (x_1,y_1)\in\Sigma_{S_0},\end{cases} \qquad (20)$$

where $\Sigma_{S_1,S_2,S_0}$ are the regions of the first interacting body surface occupied by the different kinds of roughness.

The same representation is valid for $f_2$ also,

$$f_2(x_2,y_2)=\begin{cases}-1, & (x_2,y_2)\in\tilde{\Sigma}_{S_1},\\ -\beta_1, & (x_2,y_2)\in\tilde{\Sigma}_{S_2},\\ \beta_2, & (x_2,y_2)\in\tilde{\Sigma}_{S_0},\end{cases} \qquad (21)$$

where $\tilde{\Sigma}_{S_1,S_2,S_0}$ are the regions of the second interacting body surface occupied by the distortions of different kinds.

Note that the inequality (14) is easily satisfied. For the roughness under consideration the characteristic lateral sizes of distortions are $d_p,d_s\sim 200$–$300$ nm, as can be seen from Fig. 3. At the same time $\sqrt{aR}>3000$ nm. Thus Eq. (15) is applicable for the calculation of roughness corrections.

Now it is not difficult to calculate the coefficients of expansion (15). One example is

$$\langle\langle f_1 f_2\rangle\rangle=-v_1^2-2\beta_1 v_1 v_2+2\beta_2 v_1 v_0-\beta_1^2 v_2^2+2\beta_1\beta_2 v_2 v_0 -\beta_2^2 v_0^2=0, \qquad (22)$$

which follows from Eqs. (17)–(19). The results for the other coefficients are

$$\begin{aligned}
\langle\langle f_1^2\rangle\rangle &= \langle\langle f_2^2\rangle\rangle = \nu_1+\beta_1^2\nu_2+\beta_2^2\nu_0,\\
\langle\langle f_1^3\rangle\rangle &= -\langle\langle f_2^3\rangle\rangle = \nu_1+\beta_1^3\nu_2-\beta_2^3\nu_0,\\
\langle\langle f_1 f_2^2\rangle\rangle &= \langle\langle f_1^2 f_2\rangle\rangle = 0,\\
\langle\langle f_1^4\rangle\rangle &= \langle\langle f_2^4\rangle\rangle = \nu_1+\beta_1^4\nu_2+\beta_2^4\nu_0,\\
\langle\langle f_1 f_2^3\rangle\rangle &= \langle\langle f_1^3 f_2\rangle\rangle = 0,\\
\langle\langle f_1^2 f_2^2\rangle\rangle &= (\nu_1+\beta_1^2\nu_2+\beta_2^2\nu_0)^2.
\end{aligned} \tag{23}$$

Substituting Eq. (23) into Eq. (15) we get the final expression for the Casimir force with surface distortions included up to fourth order in relative distortion amplitude,

$$\begin{aligned}
F_R(a) = F_0(a)\Bigg\{ & 1+12(\nu_1+\beta_1^2\nu_2+\beta_2^2\nu_0)\frac{A^2}{a^2}\\
& +20(\nu_1+\beta_1^3\nu_2-\beta_2^3\nu_0)\frac{A^3}{a^3}+30[\nu_1+\beta_1^4\nu_2+\beta_2^4\nu_0\\
& +3(\nu_1+\beta_1^2\nu_2+\beta_2^2\nu_0)^2]\frac{A^4}{a^4}\Bigg\}.
\end{aligned} \tag{24}$$

It should be noted that exactly the same result can be obtained in a very simple way. To do this it is enough to calculate the values of the Casimir force (12) for six different distances that are possible between the distorted surfaces, multiply them by the appropriate probabilities, and then summarize the results

$$\begin{aligned}
F_R(a) = & \sum_{i=1}^{6} w_i F_0(a_i) \equiv \nu_1^2 F_0(a-2A)\\
& +2\nu_1\nu_2 F_0(a-A(1+\beta_1))\\
& +2\nu_2\nu_0 F_0(a-A(\beta_1-\beta_2))+\nu_0^2 F_0(a+2A\beta_2)\\
& +\nu_2^2 F_0(a-2A\beta_1)+2\nu_1\nu_0 F_0(a-A(1-\beta_2)).
\end{aligned} \tag{25}$$

The question arises as to whether there is a unique definition of the distance $a$ between the interacting bodies in Eqs. (24) and (25). This point is discussed in the next section in connection with the reflectivity properties of the metals covering the plate and the sphere.

## V. CORRECTIONS TO THE CASIMIR FORCE DUE TO FINITE CONDUCTIVITY OF THE METALS

The interacting bodies used in the experiment [12] were coated with 300 nm of Al in an evaporator. The thickness of this metallic layer is much larger than the penetration depth $\delta_0$ of electromagnetic oscillations into Al for the wavelengths (sphere-plate separations) of interest. Taking $\lambda_p^{\mathrm{Al}}=100\,\mathrm{nm}$ as the approximative value of the effective plasma wavelength of the electrons in Al [28], one gets $\delta_0=\lambda_p^{\mathrm{Al}}/(2\pi)\approx 16\,\mathrm{nm}$. What this means is the interacting bodies can be considered as made of Al as a whole. Although Al reflects more than 90% of the incident electromagnetic oscillations in the complete measurement range $100\,\mathrm{nm}<\lambda<950\,\mathrm{nm}$, some corrections to the Casimir force due to the finiteness of its conductivity exist and should be taken into account. In addition, to prevent the oxidation processes, the surface of Al in [12] was covered with a $\Delta=20\,\mathrm{nm}$ layer of 60% Au/40% Pd. The reflectivity properties of this alloy are much worse than those of Al (the effective plasma wavelength of Au is $\lambda_p^{\mathrm{Au}}=500\,\mathrm{nm}$ and the penetration depth is $\tilde{\delta}_0\approx 80\,\mathrm{nm}$. Because of this, it is incorrect to use Eq. (13) to compare theory and experiment, as it is only valid for ideal metals of infinite conductivity. It is necessary to take into account the finiteness of the metal conductivity.

Let us start our discussion with the large distances $a>\lambda_p^{\mathrm{Au}}$ for which both Al and Au/Pd are the good metals. In this case the perturbation theory in the relative penetration depth can be developed. This small parameter is the ratio of an effective penetration depth $\delta_e$ (into both the Au/Pd and Al) and a distance between the Au/Pd layers $a$. The quantity $\delta_e$, in its turn, is understood as a depth for which the electromagnetic oscillations are attenuated by a factor of $e$. It takes into account both the properties of Al and of Au/Pd layers. The value of $\delta_e$ can be found from the equation

$$\frac{\Delta}{\tilde{\delta}_0}+\frac{\delta_e-\Delta}{\delta_0}=1, \quad \delta_e=\left(1-\frac{\Delta}{\tilde{\delta}_0}\right)\delta_0+\Delta\approx 32\ \ \mathrm{nm}. \tag{26}$$

The first-order correction to Eq. (13) was found in [29,30] for the configuration of two plane parallel plates. Together with the second-order correction found in [31] the result is

$$F_{\delta_e}(a)=F_0(a)\left(1-\frac{16}{3}\frac{\delta_e}{a}+24\frac{\delta_e^2}{a^2}\right). \tag{27}$$

From the general expression for $F_{\delta_e}$ it is seen that the Casimir force taking into account the finite conductivity is sign-constant for all $\delta_e$ and has a zero limit when $\delta_e\to\infty$. This gives the possibility to obtain the simple interpolation formula [31]

$$F_{\delta_e}(a)\approx F_0(a)\left(1+\frac{11}{3}\frac{\delta_e}{a}\right)^{-16/11}. \tag{28}$$

From Eq. (28) we have the same result as in Eq. (27) for small $\delta_e/a$, but it is applicable in the wider range $0\leqslant\delta_e/a\leqslant 0.2$.

Let us now expand Eq. (28) in powers of $\delta_e/a$ up to fourth order inclusive, and modify the result by the use of the force proximity theorem [27] for the case of a sphere above a plate,

$$F_{\delta_e}(a)=F_0(a)\left(1-4\frac{\delta_e}{a}+\frac{72}{5}\frac{\delta_e^2}{a^2}-\frac{152}{3}\frac{\delta_e^3}{a^3}+\frac{532}{3}\frac{\delta_e^4}{a^4}\right). \tag{29}$$

Here $F_0(a)$ is defined by Eq. (13).

Now we combine both corrections—one due to the surface roughness and the second due to the finite conductivity of the metals. For this purpose we substitute the quantity $F_{\delta_e}(a_i)$ from Eq. (29) into Eq. (25) instead of $F_0(a_i)$. The result is

$$F(a)=\sum_{i=1}^{6} w_i F_{\delta_e}(a_i), \tag{30}$$

where different possible distances between the surfaces with roughness and their probabilities were introduced in Eq. (25). Equation (30) along with Eq. (29) describe the Casimir force between Al bodies with Au/Pd layers, taking into account the finite conductivity of the metals and surface roughness for the distances $a>\lambda_p^{\mathrm{Au}}$. Note that Eq. (30) incorporates not only the corrections to the surface roughness and finite conductivity separately but also some ''crossed'' terms, i.e., the conductivity corrections to the roughness ones.

Unfortunately, Eq. (30), strictly speaking, cannot be used for the distances $a<\lambda_p^{\mathrm{Au}}$. The most rigorous way of calculating the Casimir force in this range is to apply the general Lifshitz theory without the supposition that $a$ is much larger than the characteristic absorption band of Au/Pd [this supposition leads to the result (12) with a definition (4)]. To do this detailed information is needed concerning the behavior of the dielectric permittivity of Au/Pd on the imaginary frequency axis. This information should reflect the absorption bands of the alloy and the damping of free electrons [9]. In doing so the actual dependence of the Casimir force on $a$ could be calculated, where $a$ is the distance between the outer Au/Pd layers.

At the same time, there exists a more simple, phenomenological, approach to the calculation of the Casimir force for distances less than the characteristic absorption wavelength of the Au/Pd covering. It uses the fact that the transmittance of 20-nm Au/Pd films for the wavelength of around 300 nm is greater than 90%. This transmission measurement was made by taking the ratio of light transmitted through a glass slide with and without the Au/Pd coating in an optical spectrometer.

So high transmittance gives the possibility of neglecting the Au/Pd layers when calculating the Casimir force and of enlarging the distance between the bodies by $2\Delta=40\,\mathrm{nm}$ when comparing the theoretical and experimental results. With this approach for the distances $a<\lambda_p^{\mathrm{Au}}$, instead of Eq. (30), the following result is valid:

$$F(a)=\sum_{i=1}^{6} w_i F_{\delta_0}(a_i+2\Delta), \tag{31}$$

where the Casimir force (with finite conductivity taken into account) is defined by Eq. (29).

Notice that in [32] an attempt was undertaken to numerically apply the Lifshitz theory to the test bodies made of gold, copper, or aluminum. The obtained results, however, are not applicable in our case where one metal (Al) is covered by a layer of alloy (Au/Pd). Furthermore, the above computations do not take into account surface roughness. Consequently such numerical techniques can be used only for multiplicative roughness correction, without inclusion of ''crossed'' terms (an approach that is criticized in [32]). It must also be noted that some of the conclusions made in [32] fail because of arithmetical error: the second-order plasma model leads to an overall force correction factor of 0.759, not 0.687, as is used throughout Sec. III of [32].

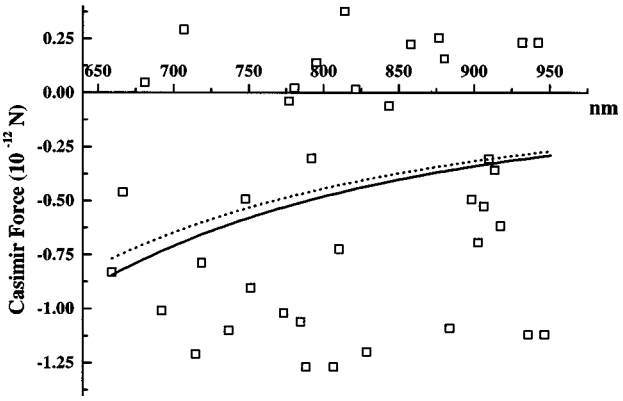


FIG. 4. Measured average Casimir force for large distances as a function of plate-sphere separation is shown as open squares. The theoretical Casimir force with corrections to surface roughness and finite conductivity is shown by the solid line (when the space separation is defined as the distance between Al layers) and by the dashed line (with the distance between Au/Pd layers).

## VI. COMPARISON WITH THE EXPERIMENT

Let us first consider large surface separations (the distance between the Au/Pd layers changes in the interval $610\,\mathrm{nm}\leqslant a\leqslant 910\,\mathrm{nm}$). We compare the results given by Eqs. (30) and (31) with experimental data. In Fig. 4 the dashed curve represents the results obtained by Eq. (30), and the solid curve those obtained by Eq. (31). The experimental points are shown as open squares. For 80 experimental points, which belong to the range of $a$ under consideration, the root-mean-square average deviation between theory and experiment in both cases is $\sigma=1.5\,\mathrm{pN}$. It is notable that for the large $a$ the same result is also valid if we use the Casimir force from Eq. (13) (i.e., without any corrections) both for $a$ and for $a+2\Delta$. By this is meant that for large $a$ the problem of the proper definition of distance is not significant due to the large scatter in experimental points due to the experimental uncertainty. The same situation occurs with the corrections. At $a+2\Delta=950\,\mathrm{nm}$ the correction due to roughness (positive) is of about 0.2% of $F_0$ and the correction due to finite conductivity (negative) is 6% of $F_0$. Together they give the negative contribution, which is also 6% of $F_0$. It is negligible if we take into account the relative error of force measurements at the extreme distance of 950 nm of approximately 660% (this is because the Casimir force is much less than the experimental uncertainty at such distances).

Now we consider the range of smaller values of the distance $80\,\mathrm{nm}\leqslant a\leqslant 460\,\mathrm{nm}$ (or, between Al, $120\,\mathrm{nm}\leqslant a+2\Delta\leqslant 500\,\mathrm{nm}$). Here Eq. (31) should be used for the Casimir force. In Fig. 5 the Casimir force $F_0(a+2\Delta)$ from Eq. (13) is shown by the dashed curve. The solid curve represents the dependence calculated according to Eq. (31). The open squares are the experimental points. Taking into account all 100 experimental points belonging to the range of smaller distances we get for the solid curve the value of the root-mean-square deviation between theory and experiment $\sigma_{100}=1.5\,\mathrm{pN}$. If we consider a more narrow distance interval of

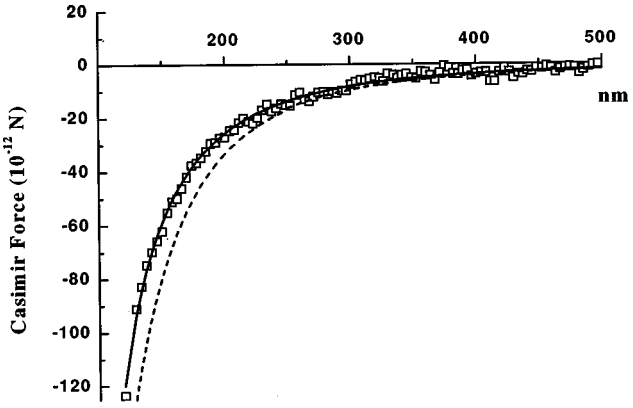


FIG. 5. Measured average Casimir force for small distances as a function of plate-sphere separation is shown as open squares. The theoretical Casimir force with corrections to surface roughness and finite conductivity is shown by the solid line, and without any correction by the dashed line.

$80\,\text{nm} \leqslant a \leqslant 200\,\text{nm}$, which contains 30 experimental points, it turns out that $\sigma_{30} = 1.6\,\text{pN}$ for the solid curve. In all the measurement range $80\,\text{nm} \leqslant a \leqslant 910\,\text{nm}$ the root-mean-square deviation for the solid curves of Figs. 4 and 5 is $\sigma_{223} = 1.4\,\text{pN}$ (223 experimental points). What this means is that the dependence (31) gives equally good agreement with experimental data in the region of small distances (for the smallest ones the relative error of force measurement is about 1%), in the region of large distances (where the relative error is rather large) and in the whole measurement range. If one uses less sophisticated expressions for the corrections to the Casimir force due to the surface roughness and finite conductivity, the value of $\sigma$ calculated for small $a$ will be larger than in the whole range [12].

It is interesting to compare the obtained results with those given by Eq. (13), i.e., without taking account of any corrections. In this case for the interval $80\,\text{nm} \leqslant a \leqslant 460\,\text{nm}$ (100 experimental points) we have $\sigma^0_{100} = 8.7\,\text{pN}$. For the whole measurement range $80\,\text{nm} \leqslant a \leqslant 910\,\text{nm}$ (223 points) there is $\sigma^0_{223} = 5.9\,\text{pN}$. It is evident that without appropriate treatment of the corrections to the Casimir force the value of the root-mean-square deviation is not only larger but also depends significantly on the measurement range.

The comparative role of each correction is also quite obvious. If we take into account only roughness correction according to Eq. (25), then one obtains for the root-mean-square deviation in different intervals: $\sigma^R_{30} = 22.8\,\text{pN}$, $\sigma^R_{100} = 12.7\,\text{pN}$, and $\sigma^R_{223} = 8.5\,\text{pN}$. At $a + 2\Delta = 120\,\text{nm}$ the correction is 17% of $F_0$. For the single finite conductivity correction calculated by Eq. (29) with $\delta_0$ instead of $\delta_e$ it follows that $\sigma^\delta_{30} = 5.2\,\text{pN}$, $\sigma^\delta_{100} = 3.1\,\text{pN}$, and $\sigma^\delta_{223} = 2.3\,\text{pN}$. At 120 nm this correction contributes $-34\%$ of $F_0$. (Note, that both corrections contribute $-22\%$ of $F_0$ at 120 nm, so that their nonadditivity is demonstrated most clearly.)

Considering the case of small distances, we have neglected the contribution of thin Au/Pd layers that are almost transparent for the essential frequencies. The corrections to the Casimir force due to these layers can be calculated by considering them as being made of some effective dielectric with a small permittivity $\varepsilon$ [5]. Such corrections calculated with $\varepsilon \approx 1.1$ lead, together with Eq. (31), to the same value of $\sigma$ if we increase the values of all distances by 1 nm. If the effective value of permittivity would be $\varepsilon \approx 1.2$ this is equivalent to the addition of 3 nm to all the distances without changing of $\sigma$. As can well be imagined, the corrections due to Au/Pd layers are not essential when it is considered that the absolute uncertainty of distance measurements in the experiment [12] was about $\pm 5$ nm.

## VII. CONCLUSIONS AND DISCUSSION

In the above, the surface roughness of the test bodies used in the experiment [12] on Casimir force measurement was investigated with the use of AFM and SEM. The corrections to this force due to both surface roughness and finite conductivity of the metal were calculated up to fourth order in respective small parameters. The obtained theoretical results for the Casimir force with both corrections were compared with the experimental data. Excellent agreement was demonstrated that is characterized by almost the same value of the root-mean-square deviation between theory and experiment in the cases of small and large space separations between the test bodies and in the complete measurement range.

It was shown that the agreement between theory and experiment is substantially worse if any one of the corrections is not taken into account. What this means is that the surface roughness and finite conductivity corrections should be taken into account in precision Casimir force measurements with space separations of the order 1 $\mu$m and less. They will also be expected to play a strong role in experimental tests of the shape and topology dependences of the Casimir force.

Further improvements in the precision can be achieved through the use of smoother metallic coatings, thinner Au layers (but of enough thickness to prevent the oxidation processes of Al), and larger radius spheres to increase the values of force. The experimental uncertainties can be substantially reduced by use of lower temperatures to decrease the thermal noise in the AFM, and interferometric detection of cantilever deflection [33]. This will provide the opportunity to increase the accuracy of Casimir force measurements and to obtain stronger constraints on the constants of hypothetical long-range interactions and light elementary particles. Such constraints for the different ranges of Compton wavelengths of hypothetical particles were already obtained in [34] from the experiment [10] and in [35] from the experiment [12]. There is reason to hope that within the next few years the Casimir effect will become a strong competitor of the more traditional physical phenomena, which can provide us with new data about long-range interactions and light elementary particles.

## ACKNOWLEDGMENT

G.L.K. and V.M.M. are grateful to the Physics Department of the Federal University of Paraíba, where this work was partly done, for their kind hospitality.

[1] H. B. G. Casimir, Proc. K. Ned. Akad. Wet. **51**, 793 (1948).
[2] G. Plunien, B. Müller, and W. Greiner, Phys. Rep. **134**, 87 (1986).
[3] V. M. Mostepanenko and N. N. Trunov, Usp. Fiz. Nauk **156**, 385 (1988) [Sov. Phys. Usp. **31**, 965 (1988)].
[4] P. W. Milonni, *The Quantum Vacuum* (Academic Press, San Diego, 1994).
[5] V. M. Mostepanenko and N. N. Trunov, *The Casimir Effect and Its Applications* (Clarendon Press, Oxford, 1997).
[6] M. J. Sparnaay, Physica (Amsterdam) **24**, 751 (1958).
[7] D. Tabor and R. H. S. Winterton, Proc. R. Soc. London, Ser. A **312**, 435 (1969).
[8] S. Hunklinger, H. Geisselmann, and W. Arnold, Rev. Sci. Instrum. **43**, 584 (1972).
[9] P. H. G. M. van Blokland and J. T. G. Overbeek, J. Chem. Soc., Faraday Trans. 1 **74**, 2637 (1978).
[10] S. K. Lamoreaux, Phys. Rev. Lett. **78**, 5 (1997); **81**, 5475 (1998).
[11] G. L. Klimchitskaya and Yu. V. Pavlov, Int. J. Mod. Phys. A **11**, 3723 (1996).
[12] U. Mohideen and A. Roy, Phys. Rev. Lett. **81**, 4549 (1998).
[13] V. B. Bezerra, G. L. Klimchitskaya, and C. Romero, Mod. Phys. Lett. A **12**, 2613 (1997).
[14] R. Onofrio and G. Carugno, Phys. Lett. A **198**, 365 (1995).
[15] A. Grado, E. Calloni, and L. Di Fiore, Phys. Rev. D **59**, 042002 (1999).
[16] V. M. Mostepanenko and I. Yu. Sokolov, Dokl. Akad. Nauk SSSR **298**, 1380 (1988) [Sov. Phys. Dokl. **33**, 140 (1988)].
[17] M. Bordag, G. L. Klimchitskaya, and V. M. Mostepanenko, Int. J. Mod. Phys. A **10**, 2661 (1995).
[18] W. R. Smythe, *Electrostatics and Electrodynamics* (McGraw-Hill, New York, 1950).
[19] J. L. M. J. van Bree, J. A. Poulis, B. J. Verhaar, and K. Schram, Physica (Amsterdam) **78**, 187 (1974).
[20] M. Bordag, G. L. Klimchitskaya, and V. M. Mostepanenko, Phys. Lett. A **200**, 95 (1995).
[21] A. A. Maradudin and P. Mazur, Phys. Rev. B **22**, 1677 (1980).
[22] P. Mazur and A. A. Maradudin, Phys. Rev. B **23**, 695 (1981).
[23] E. M. Lifshitz and L. P. Pitaevskii, *Statistical Physics, Part 2* (Pergamon Press, Oxford, 1980).
[24] M. Schaden and L. Spruch, Phys. Rev. A **58**, 935 (1998).
[25] L. H. Ford, Phys. Rev. A **58**, 4279 (1998).
[26] R. Golestanian and M. Kardar, Phys. Rev. A **58**, 1713 (1998).
[27] J. Blocki, J. Randrup, W. J. Swiatecki, and C. F. Tsang, Ann. Phys. (N.Y.) **105**, 427 (1977).
[28] *Handbook of Optical Constants of Solids*, edited by E. D. Palik (Academic Press, New York, 1985).
[29] C. M. Hargreaves, Proc. K. Ned. Akad. Wet., Ser. B: Phys. Sci. **68**, 231 (1965).
[30] J. Schwinger, L. L. DeRaad, Jr., and K. A. Milton, Ann. Phys. (N.Y.) **115**, 1 (1978).
[31] V. M. Mostepanenko and N. N. Trunov, Yad. Fiz **42**, 1297 (1985) [Sov. J. Nucl. Phys. **42**, 818 (1985)].
[32] S. K. Lamoreaux, Phys. Rev. A **59**, R3149 (1999).
[33] T. Stowe, K. Yasumura, T. W. Kenny, D. Botkin, K. Wago, and D. Rugar, Appl. Phys. Lett. **71**, 288 (1997).
[34] M. Bordag, B. Geyer, G. L. Klimchitskaya, and V. M. Mostepanenko, Phys. Rev. D **58**, 075003 (1998).
[35] M. Bordag, B. Geyer, G. L. Klimchitskaya, and V. M. Mostepanenko, Phys. Rev. D **60**, 055 004 (1999).